PAPER Special Section on Smart Multimedia & Communication Systems

Timing Synchronization Performance of Short Preamble Sequence with Orthogonal Frequency Multiplexed Data Symbols

Yuki TANAKA[†a)], ***Student Member and*** **Yukitoshi SANADA**[†b)], ***Senior Member***

SUMMARY Wireless communications for the control of industrial equipments need to send a large amount of short packets frequently and to improve frame efficiency. The OFDM frame of wireless local area networks has short preambles that are used for timing synchronization and coarse frequency offset estimation. As the short preambles are repeated in a time domain, they occupies subcarriers intermittently. Therefore, in this paper, a new frame format with OFDM modulation in which data symbols are orthogonally multiplexed with the preamble symbols in the frequency domain is proposed. Two preamble sequences that are based on an IEEE802.11g short preamble sequence and a Zadoff-Chu sequence are examined. The ratio of transmission powers between the pilot subcarrier and the data subcarrier is also varied. The timing synchronization probability with those sequences has been evaluated on different channel models. It is shown through the experiment that the synchronization performance is almost the same as that without data multiplexing at E_s/N_0 of more than 8 dB.

key words: *M2M, timing synchronization, OFDM*

1. Introduction

Recently wireless communications for Machine-to-Machine (M2M) applications have been investigated [1]. M2M communications have various applications including environmental monitoring, public safety, health care, and so on. One of the applications for M2M wireless communications is industrial automation [2].

Wireless communications for the control of industrial equipments need to frequently send a large amount of short packets and it is required to improve frame efficiency [3]. To realize high frame efficiency, the period of a preamble sequence that is used for the demodulation of a received signal has to be shorten [4], [5]. However, it is hard for a random access system since the preamble is also used for the adjustment of analog circuits [6].

On the other hand, M2M communications have various applications and they might be implemented in severe multipath environments with a large delay spread [7]. An orthogonal frequency division multiplexing (OFDM) scheme is robust to severe multipath channels. Accurate synchronization of the OFDM signal is required to prevent inter-carrier interference (ICI) and to improve demodulation performance [8].

In order to shorten the preamble period and improve the frame efficiency, a new frame format in which data symbols are orthogonally multiplexed with the preambles in the frequency domain is proposed in this paper. Two types of preamble signals are proposed and their synchronization performance is evaluated. One is based on an IEEE802.11g short preamble sequence [9]. The frequency spectrum of the 11g short preamble has a margin at the channel edge to the spectrum mask specified in the IEEE802.11g standard. Another is based on a Zadoff-Chu sequence which has higher packet utilization efficiency than the IEEE802.11g short preamble. Ths frequency spectrum of the Zadoff-Chu sequence based preamble spans over the whole spectrum mask. Thus, it can carry more data symbols while the larger frequency interval of pilot subcarriers effects on the accuracy of channel estimation. The synchronization probability and the BER performance of the preambles multiplexed with data symbols are evaluated through the experiment in this paper.

This paper is organized as follows. Our experiment system is explained in Sect. 2. Numerical results obtained through the experiment are shown in Sect. 3. Finally, conclusions are presented in Sect. 4.

Notation: Throughout the paper, a variable expressed with a capital letter implies a quantity in a frequency domain while a variable represented with a small letter indicates a quantity in a frequency domain.

2. Experiment System

2.1 Measurement Setup

Figure 1 illustrates a block diagram of the experiment system. The transmitter and the receiver are connected by a cable in this experiment system. An OFDM signal following the IEEE802.11g format is generated by the signal generator. Table 1 shows the specifications of measurement equipments. The received signal is downconverted and digitized in the Sora radio control board (RCB) that is a software defined radio platform [10]. The digital samples are stored in the memories on the personal computer (PC). The PC picks

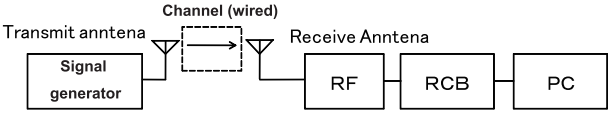

Fig. 1 Experiment system.

Manuscript received January 30, 2014.
Manuscript revised June 20, 2014.

[†]The authors are with the Dept. of Electronics and Electrical Engineering, Keio University, Yokohama-shi, 223-8522 Japan.
a) E-mail: ytanaka@snd.elec.keio.ac.jp
b) E-mail: sanada@elec.keio.ac.jp

DOI: 10.1587/transfun.E97.A.2097

Table 1 Measurement equipment.

ESG Vector Signal Generator Agilent "E4438C"	Frequency: from 250 kHz to 6 GHz Maximum Output Power: +17 dBm
RF Transceiver MAXIM "MAX2829"	Frequency: 2.4 GHz-2.5 GHz 4.9–5.875 GHz Gain Control Range : 93 dB Dynamic Range: 60 dB
A/D Converter ANALOG DEVICES "AD9248"	Speed: 20 Msymbol/s, 40 Msymbol/s, 65 Msymbol/s Resolution: 14 bit
Personal Computer Intel Core i7 930	Clock: 2.8 GHz Core: Quad Core

Table 2 Specifications of signal.

Bandwidth of the Channel	20 MHz
Center Frequency of the Channel	2.442 GHz
Modulation Scheme	OFDM
Size of DFT	64
Number of Subcarriers	52 (IEEE802.11g short preamble) 56 (Zadoff-Chu sequence)
Number of Data Subcarriers	40(IEEE802.11g short preamble) 48(Zadoff-Chu sequence)
Short Preamble Duration	0.8 μs
Cyclic Prefix Duration	0.8 μs
Symbol Duration	3.2 μs
Transmit Power	−20 dBm (with 20 dB attenuator)

up the stored samples and carries out carrier detection continuously.

2.2 Transmit Signal

The specifications of the OFDM signal used for the experiment are shown in Table 2 [9]. The OFDM signal is generated with the clock speed of 20 MHz. The number of subcarriers used for the preamble and data signals is 52 while the size of the DFT is N=64. The bandwidth of the signal is $1/T_s$=20 MHz where T_s is the sampling interval of the OFDM signal. The frequency response of the filter is shown in Fig. 2. This filter follows the IEEE802.11g spectrum mask. It is assumed here that a half of the preamble period is used for the detection of a carrier signal as well as the adjustment of an RF front end and following analog circuits [12]. For simplicity, it is assumed that the adjustment process of the RF circuits is carried out during the first half of the preamble period and analog-to-digital (A/D) conversion starts from the last half of the preamble period that carries the data signal as well as the cyclic prefix.

2.3 Frame Format

Two types of the preamble sequence is employed in this paper. One is the short preamble sequence with the length of 16 points specified in the IEEE802.11g standard and another one is the Zadoff Chu sequence with the length of 8 points. The whole preamble period is 160, the DFT size is 64, and the cyclic prefix size is 16. Thus, the preamble sequence is

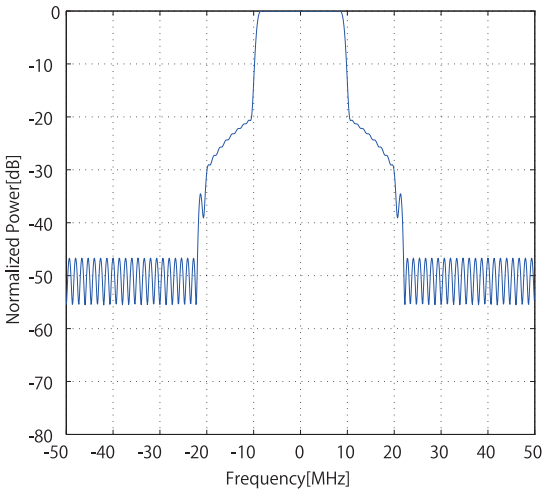

Fig. 2 Frequency response of transmit filter.

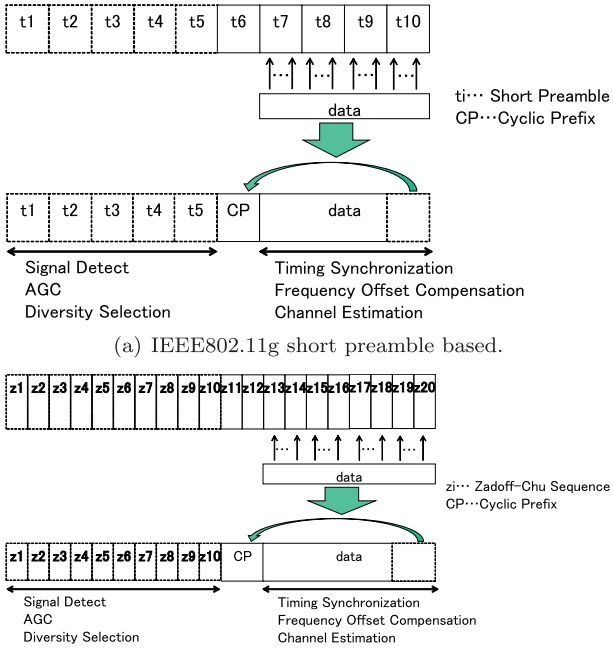

(a) IEEE802.11g short preamble based.

(b) Zadoff-Chu sequence based.

Fig. 3 Transmit signal format.

repeated 10 times in the IEEE802.11g short preamle based frame while it is repeated 20 times in the the Zadoff Chu sequence based frame as shown in Figs. 3(a) and 3(b).

2.3.1 IEEE802.11g Short Preamble Based Frame

The short preamble sequence specified in the IEEE802.11g standard spans over 12 subcarriers with the interval of 4 subcarriers in the frequency domain. An example of the power spectrum density of the transmit signal with the IEEE802.11g short preamble sequence is shown in Fig. 4. The ratio of the powers between the data subcarrier and the pilot subcarrier is 1:8 in this example. The notable thing of this sequence is that this sequence does not contain the

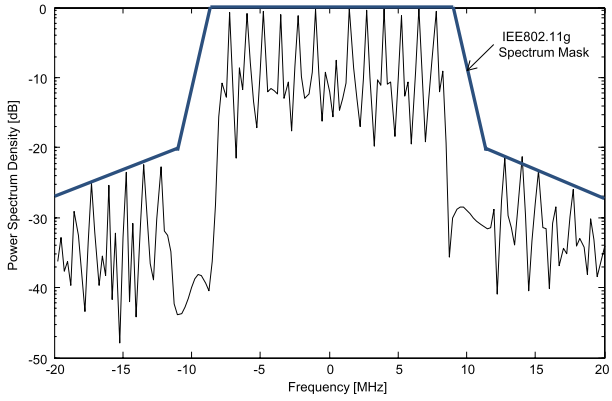

Fig. 4 Frequency spectrum of IEEE802.11g short preamble sequence based frame (Power ratio = (1:8)).

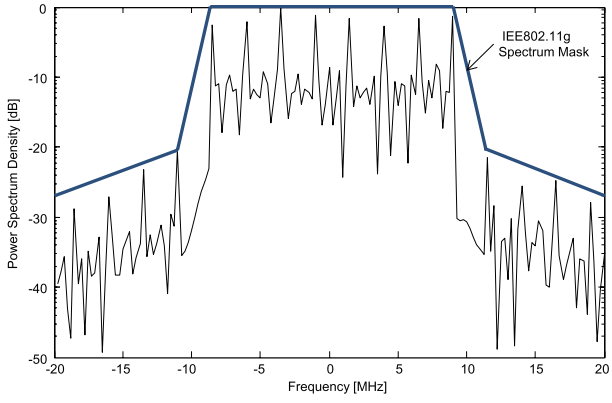

Fig. 5 Frequency spectrum of Zadoff-Chu sequence based frame (Power ratio = (1:8)).

frequency component at the channel edge even though it is repeated 4 times over one OFDM symbol duration. Thus, there is a margin between the edge of the signal spectrum and the spectrum mask. In this frame format, following the IEEE802.11g standard, 52 subcarriers including 12 pilot subcarriers and 40 data subcarriers are used for data transmission.

2.3.2 Zadoff-Chu Sequence Based Preamble

The Zadoff-Chu sequence is a complex-valued mathematical sequence which realizes an electromagnetic signal of constant amplitude [11]. The Zadoff-Chu sequence with the length of 8 points is repeated 8 times over one OFDM symbol duration in the time domain and it spans over 8 subcarriers with the interval of 8 subcarriers in the frequency domain. An example of the power spectrum density of the transmit signal with the Zadoff-Chu sequence is shown in Fig. 5. The ratio of the powers between the data subcarrier and the pilot subcarrier is 1:8 in this example. The Zadoff-Chu sequence can be designed for any length. However, it can not be fit in the IEEE802.11a spectrum mask if the sequence length is longer. If the sequence length is shorter, the interval between the auto-correlation peaks reduces. On the other hand, the larger frequency interval of pilot subcarriers effects on the accuracy of channel estimation. Thus, in this experiment, the Zadoff-Chu sequence with the length of 8 points is employed for evaluation. Since the power spectrum of the transmit signal satisfies the spectrum mask, 56 subcarriers including 8 pilot subcarriers and 48 data subcarriers are used for data transmission.

2.4 OFDM Symbol

The OFDM symbols in the last half of the preamble period is expressed as follows. Suppose that the symbol on the kth subcarrier is $X[k]$ ($k = -\frac{N}{2},...,-\frac{N}{2}-1$), the nth OFDM signal in the time domain, $x[n]$, is given as

$$x[n] = \frac{1}{N}\sum_{k=-\frac{N}{2}}^{\frac{N}{2}-1} X[k]\exp\left(j2\pi\frac{nk}{N}\right) \tag{1}$$

where k is the subcarrier index, n (n= 0, ..., $N-1$) is the time index, and N indicates the number of subcarriers. The preamble symbols are C times repeated over the OFDM symbol duration in the time domain. This implies that they are transmitted on every C subcarriers in the frequency domain. The subcarrier indexes for the preamble symbols are given as follows

$$k_p = \begin{cases} C(k'-1)+4+N/2, & k' = 1, 2, ..., D \\ C(k'+1)-4+N/2, & k' = -1, -2, ..., -D \end{cases} \tag{2}$$

where $2D$ is the number of the preamble symbols and is 12 or 8 and C is set to 4 or 8 for the 11g short preamble or the Zadoff-Chu sequence, respectively. The preamble symbols and the data symbols are multiplexed in the frequency domain as shown in Fig. 6. It is orthogonally transmitted over the subcarriers of $-26 \le k \le 26$ for the 11g short preamble sequence or of $-28 \le k \le 28$ for the Zadoff-Chu sequence based preamble except $k \in \{k_p\}$ (preamble subcarriers) and $k = 0$ (DC subcarrier). If the cyclic prefix (CP) is applied to the symbol, the last part of the symbol is repeated at the beginning as follows.

$$x(t) = \sum_{n=0}^{N+N_c-1} x[n]p_t(t - nT_s) \tag{3}$$

where N_c is the cyclic prefix duration and $p_t(t)$ is the impulse response of the transmit filter. The last half of the preamble symbols then consists of $(N + N_c)$ samples given in Eq. (3).

Finally, the filtered signal is transmitted in the 2.4 GHz band from the signal generator. As channel models an AWGN channel and indoor multipath fading channels are assumed and generated in the signal generator [13]. Two different multipath channels, Indoor Residential A and Indoor Office C, are assumed in the experiment. This is because the RMS delay of the wireless channels in the M2M applications spans from tens of nano seconds to 1 micro second [7]. The delay profiles of the Indoor Residential A model

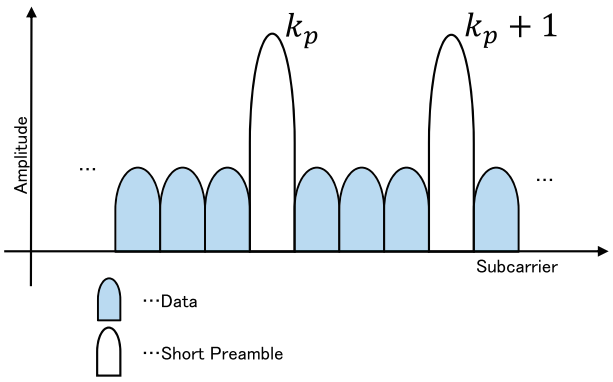

Fig. 6 Multiplexing preamble and data symbols in frequency domain.

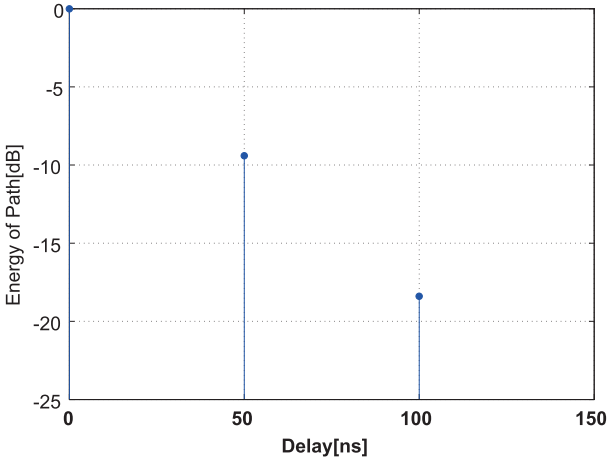

Fig. 7 Delay profile of Indoor Residential A channel model.

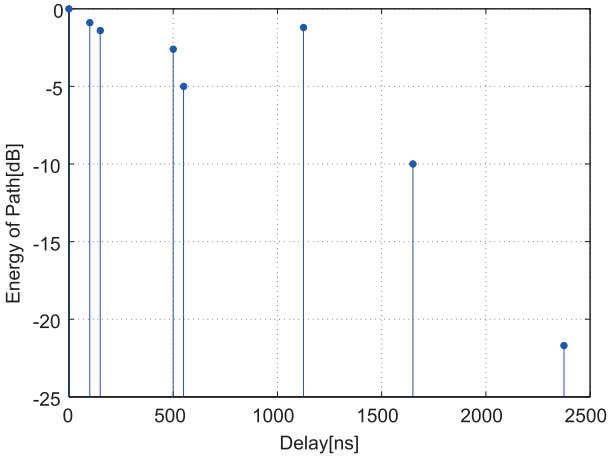

Fig. 8 Delay profile of Indoor Office C channel model.

and the Indoor Office C model used in the experiment are shown in Figs. 7 and 8, respectively.

2.5 Signal Processing in Receiver

The block diagram of the receiver programmed on the PC is shown in Fig. 9. After downconversion, the received signal

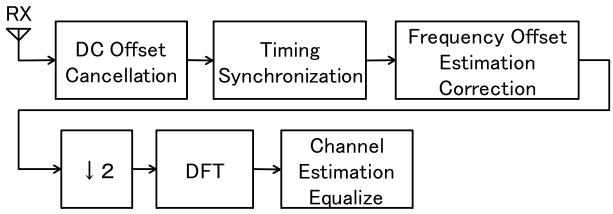

Fig. 9 Block diagram of signal processing in receiver.

is sampled at the rate of 40 MHz. The DC offset of the received signal is first removed and timing synchronization is carried out. The frequency offset of the received signal is estimated and removed with the preamble symbols. After downsampling, the OFDM signal passes through the DFT block. The data symbols multiplexed in the frequency domain is then demodulated after channel estimation and equalization on each subcarrier.

2.5.1 DC Offset Cancelation

The DC offset of the received signal, $\hat{o}$, is estimated with the following equation.

$$\hat{o} = \frac{\sum_{n=1}^{M} y[n]}{M} \tag{4}$$

where $y[n]$ is the nth sample of the received signal and M is the number of the samples available for averaging. The averaging is carried out every 512 samples, i.e. $M = 512$. DC offset cancelation can be carried out by subtracting $\hat{o}$ from the received samples as follows.

$$\hat{y}[n] = y[n] - \hat{o}, \qquad n = 1, 2..., N \tag{5}$$

where $\hat{y}[n]$ is the nth sample after DC offset cancelation.

2.5.2 Timing Synchronization

The timing synchronization scheme employs matched filtering to the preamble symbols [14]. The filter length is 5 short preamble symbol duration. The ith output of the correlator, $p[i]$, is given as follows.

$$p[i] = \sum_{n=0}^{5CN_s/4-1} \hat{y}[i+n] s_s^*[n \mod N_s] \tag{6}$$

where $s_s[i]$ is the ith sample of the preamble symbols and N_s is the length of one short preamble, i.e., $N_s = 32$ for the 11g short preamble and $N_s = 16$ for the Zadoff-Chu sequence based preamble with 2 times oversampling. The peak output of the matched filter is detected with the output of the correlator and then the synchronization timing is decided.

2.5.3 Frequency Offset Cancelation

A frequency offset is estimated with the last five short preamble symbols in which data symbols are multiplexed in the frequency domain. Matched filtering is applied to these

short preambles and the frequency offset is estimated. The length of the matched filter is set to one OFDM symbol duration and two or four auto-correlation peaks for $C = 4$ or $C = 8$ appear at the outputs with the interval of N_s samples. The lth output of the correlator with the short preamble symbols can be expressed as

$$q[l] = \sum_{n=C(l-1)N_s/4}^{(4+(l-1))CN_s/4-1} \hat{y}[n]s_s^*[n], \qquad l = 1, 2 \tag{7}$$

where the packet frame is assumed here to start from n=0. The estimation of the frequency offset, α_s, is given as

$$\alpha_s = \frac{1}{2\pi CN_s/4} \arg\left(q^*[1]q[2]\right). \tag{8}$$

In this way, the estimation of the frequency offset is obtained and tentative cancelation is carried out to the preamble symbols in which data symbols are multiplexed as follows.

$$\tilde{y}[n] = \hat{y}[n] \exp\left(j2\pi\alpha_s n\right), \qquad n = 0, 1, ... \tag{9}$$

where $\tilde{y}[n]$ is the nth received sample after the tentative cancelation of the frequency offset.

2.5.4 Channel Equalization and Demodulation

After DC offset cancelation, timing synchronization, and frequency offset compensation, the received signal is downsampled with the ratio of 2. Following the downsampling, those samples are put into the DFT block. The received signal after downsampling, $\tilde{\tilde{y}}[n]$, is given as follows.

$$\tilde{\tilde{y}}[n] = \tilde{y}[2n]. \tag{10}$$

The received signal on the kth subcarrier is obtained through the following equation,

$$Z[k] = \sum_{n=N_{GI}+1}^{N+N_{GI}} \tilde{\tilde{y}}[n] \exp\left(j2\pi\frac{kn}{N}\right), \tag{11}$$

where $Z[k]$ is the received signal on the kth subcarrier. The channel estimation with the pilot subcarrier, k_p, is carried out as

$$\hat{H}[k_p] = Z[k_p]{S_p}^{-1}[k_p] \tag{12}$$

where $\hat{H}[k_p]$is the channel response and $S_p[k_p]$ is the short preamble symbol on the k_pth subcarrier, respectively. The channel responses between the k_pth and $(k_p + C)$th subcarriers are estimated by linear interpolation as follows.

$$\hat{H}[k] = \hat{H}[k_p] + (k - k_p)\frac{\hat{H}[k_p + C] - \hat{H}[k_p]}{C}. \tag{13}$$

Equation (12) only covers the subcarriers with the subcarrier indexes of $4 < |k| < C(D-1) + 4$ for $-4 < k < +4$, the channel responses are estimated by linear extrapolation.

With the estimated channel response, the received symbols are equalized through a Zero-Forcing algorithm. The demodulated symbol on the kth subcarrier after channel equalization is given as

$$\hat{S}[k] = \hat{H}^{-1}[k]Z[k] \tag{14}$$

where $\hat{S}[k]$ is the data symbol on the kth subcarrier after channel equalization, $\hat{H}$ is the estimated channel response. Information bits are then demodulated with $\hat{S}[k]$.

3. Measurement Results

Table 3 shows the measurement conditions. RF and baseband gains are set to 16 and 8 dB in order to make the received signal fit in the range of the A/D converters since no gain control function is implemented. The synchronization performance and the BER of the proposed scheme are evaluated in term of E_s/N_0 where E_s is the energy per sample while N_0 is the noise spectrum density. E_s/N_0 is measured in the SORA receiver side by comparing the average power of the received signal samples with and without the transmit signal including the data signal. It is varied by changing the power of the transmit signal from the signal generator. For the measurement of the synchronization probability a pseudo noise sequence with the length of 127 is appended prior to the OFDM frame to give the reference synchronization timing point. In the measurements on the multipath fading channel models, the synchronization range is set to ±300ns to the reference, in which synchronization is assumed to be realized [12]. The ratio of transmission powers between the pilot subcarrier and the data subcarrier is varied in this measurement. The ratios are set to (1:1), (1:2), (1:4,6), (1:8), or (1:16). Numerical evaluation obtained through computer simulation has also been included in performance graphs as reference and those curves are indicated with dashed lines while the numerical results obtained through the experiments are presented with solid lines. In general, the synchronization probability with the experiments exceeds that with computer simulation in terms of the synchronization probability. The reason is that no residual interference component owing to the DC offset after the DC offset cancelation is assumed in the computer simulation. The same tendency has been observed in the experiment with the same equipment in [15]. Though it is particularly significant if the power of the noise is relatively

Table 3 Measurement conditions.

Modulation Scheme	BPSK
RF gain	16 [dB]
Base band gain	8 [dB]
Transmit Power	0 dBm [dBm/20 MHz]
Channel models	Indoor Residential A Indoor Office C
Power Ratio (Data vs. Pilot)	1:1 1:2 1:4.6 1:8 1:16
Number of Trials	10000

large as compared to the peak output of the correlator because of the residual DC offset, the experiment results coincide with the simulation results in the high synchronization probability region in the following performance graphs.

3.1 Synchronization Probability

3.1.1 IEEE802.11g Short Preamble

Figures 10, 11 show the synchronization probability with the 11g short preamble on different channel models. From Figs. 10, 11, if the power of the pilot subcarrier is larger, the synchronization performance improves. This is because the output of the correlator increases with the larger power of the pilot symbols under the same E_s/N_0 condition. In Fig. 10, the synchronization performance with the power ratio of (Data:Pilot) = (1:8) is close to that with no data symbols when E_s/N_0 is more than 8 dB on the Indoor Residential A channel model. When the Indoor Office-C channel model is selected, the synchronization performance is deteriorated and never exceeds 0.8 as shown in Fig. 11. Since the Indoor Office-C channel model has a delay spread which is larger than the CP of the transmit signal, the degradation is caused by the ISI.

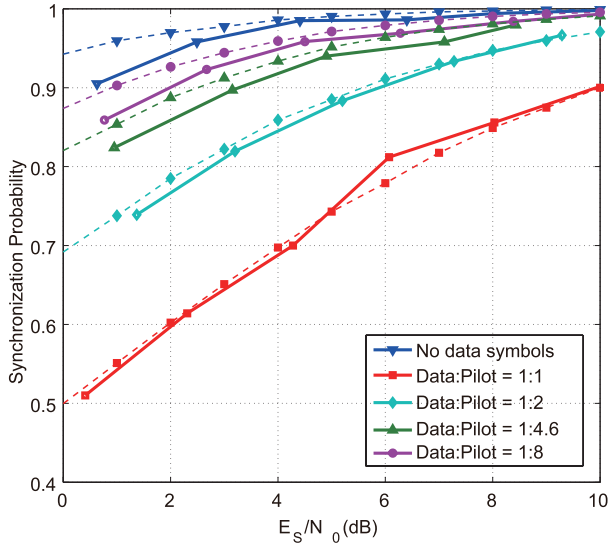

Fig. 10 Synchronization probability vs. E_s/N_0 (11g short preamble, Indoor Residential A channel model).

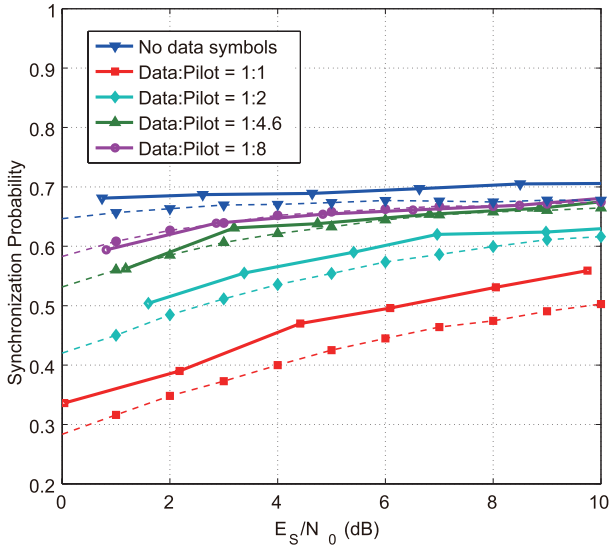

Fig. 11 Synchronization probability vs. E_s/N_0 (11g Short Preamble, Indoor Office C channel model).

3.1.2 Zadoff-Chu Sequence

Figures 12, 13 show the synchronization probability with the Zadoff-Chu sequence on different channel models. From

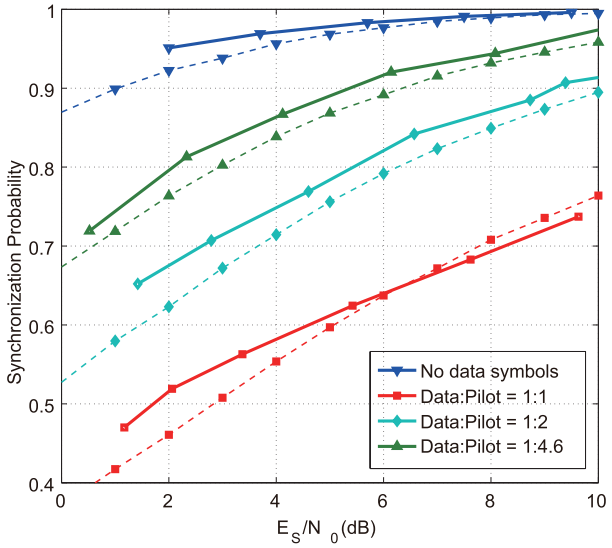

(a) Power ratio of (1:1), (1:2), and (1:4.6).

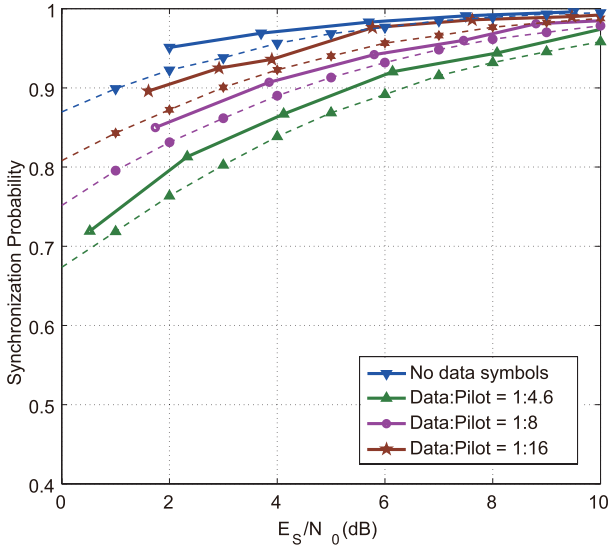

(b) Power ratio of (1:4.6), (1:8), and (1:16).

Fig. 12 Synchronization probability vs. E_s/N_0 (Zadoff-Chu sequence, Indoor Residential A channel model).

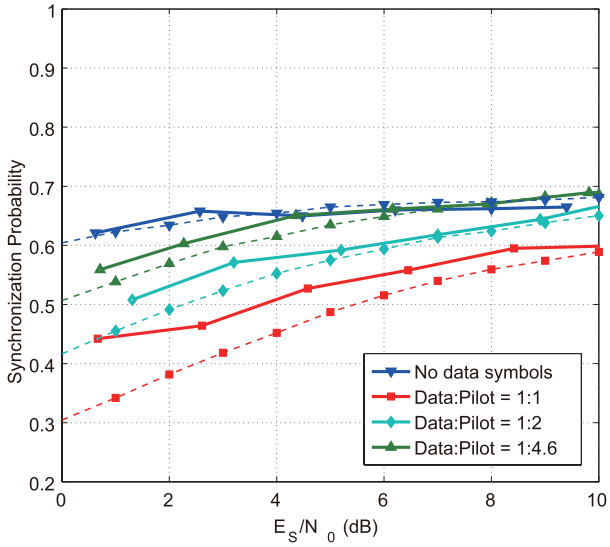

(a) Power ratio of (1:1), (1:2), and (1:4.6).

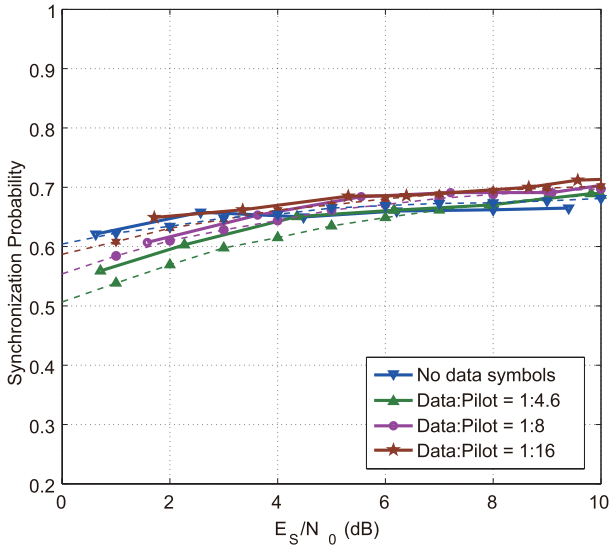

(b) Power ratio of (1:4.6), (1:8), and (1:16).

Fig. 13 Synchronization probability vs. E_s/N_0 (Zadoff-Chu sequence, Indoor Office C channel model).

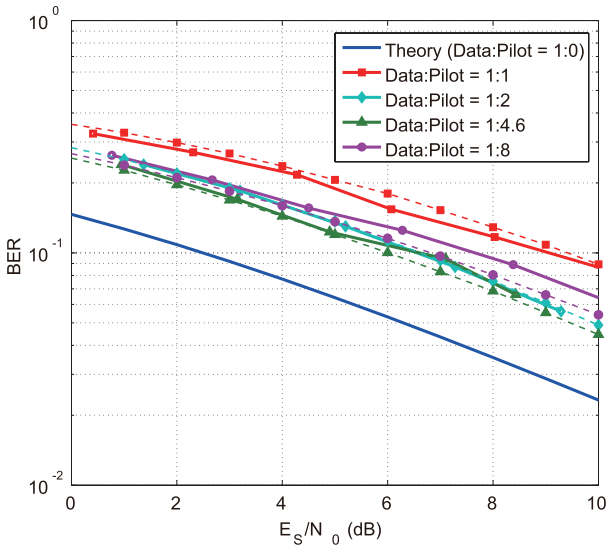

Fig. 14 BER vs. E_s/N_0 (11g short preamble, Indoor Residential A channel model).

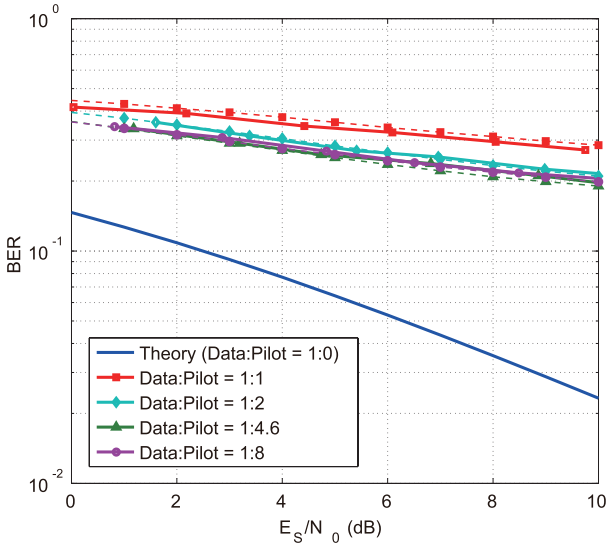

Fig. 15 BER vs. E_s/N_0 (11g short preamble, Indoor Office C channel model).

Figs. 12, 13, if the power of the pilot subcarrier grows, the synchronization performance improves. This is because the output of the correlator increases with the larger power of the pilot symbols under the same E_s/N_0 condition. In Fig. 12, the synchronization performance with the power ratio of (Data:Pilot) = (1:16) is close to that with no data symbols when E_s/N_0 is more than 8 dB on the Indoor Residential A channel model.

Comparing to the performance for the 11g short preamble, the synchronization performance for the Zadoff-Chu sequence shows about 2 dB degradation. This is because the pilot subcarriers of the Zadoff-Chu sequence has the less amount of the power due to the smaller number of the pilot subcarriers under the same E_s/N_0 condition than that of the 11g short preamble.

3.2 BER Performance

3.2.1 IEEE802.11g Short Preamble

Figures 14, 15 show the BER performance vs. E_s/N_0. E_b/N_0 can be calculated from E_s/N_0, the numbers of the pilot and data subcarreirs, and the power ratio between the pilot and data subcarriers. E_s can be converted to the bit energy E_b as follows.

$$E_b = E_s \frac{NP_d}{P_p N_p + P_d N_d} \tag{15}$$

where N_p is the number of the pilot subcarriers, N_d is the number of the data subcarriers, and P_p or P_d is the power

of the pilot symbol or data symbol, respectively. In those figures, "Theory" indicates the theoretical curve of the BER on the Rayleigh fading channel. In Figs. 14, 15, the power ratio of $(P_d : P_p) = (1 : 4.6)$ achieves the best performance on the multipath channel model. The reason is that the channel estimation error increases more on the multipath fading channel and the larger power on the pilot subcarriers is required. If the power ratio increases and the pilot subcarriers occupy a larger part of the transmission power, the bit energy reduces as given in Eq. (15). If the power ratio decreases and the pilot subcarriers consume less transmission power, the channel estimation error increases. Thus, there is a tradeoff between the powers of the pilot subcarriers and the data subcarriers. From Fig. 14, the BER performance of the power ratio of $(P_d : P_p) = (1 : 4.6)$ shows about 4 dB degradation as compared to the theoretical curve on the Indoor Residential A channel model. This is because the theoretical curve does not assume the pilot symbols and the power of the data symbols in the theoretical curve is higher with the same E_s/N_0 condition. The channel estimation error also increases the BER. In Fig. 15, the BER performance shows the severe degradation as compared to the theoretical curve on the Indoor Office C channel model. This is because of the low synchronization probability as shown in Figs. 11 and 13.

3.2.2 Zadoff-Chu Sequence

Figures 16, 17 show the BER performance vs. E_s/N_0. In Figs. 16, 17, the power ratio of $(P_d : P_p) = (1 : 4.6)$ or $(1 : 8)$ realizes the best BERs on the multipath channel models. This is because the interval between the pilot subcarriers is larger in the Zadoff-Chu sequence based preamble. From Fig. 16, the BER performance of the power ratio of $(P_d : P_p) = (1 : 4.6)$ or $(1 : 8)$ has about 4 dB degradation as compared to the theoretical curve on the Indoor Residential A channel model. While the synchronization probability of the the Zadoff-Chu sequence based preamble is worse than that with the 11g short preamble because of the smaller because of the smaller power assignment to the pilot subcarriers, bit energy is about 1.1 dB larger for the same E_s/N_0 and the same power ratio. Since the BER evaluation includes the errors due to the timing synchronization loss, the BER curves with the 11g preamble and the the Zadoff-Chu sequence based preamble shows almost the same performance when the power ratio is $(1 : 4.6)$.

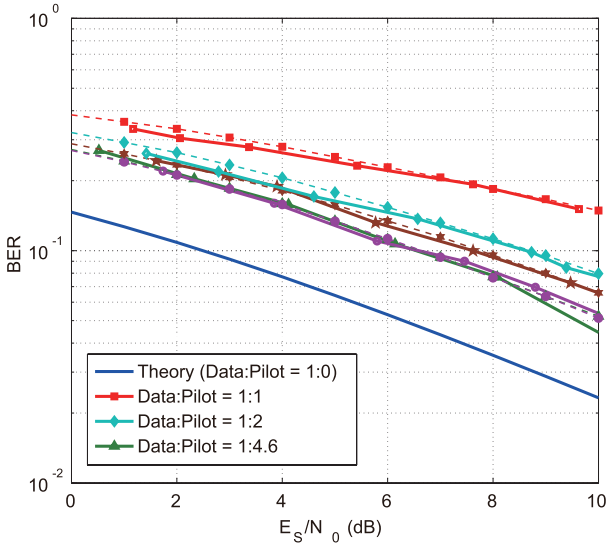

(a) Power ratio of (1:1), (1:2), and (1:4.6).

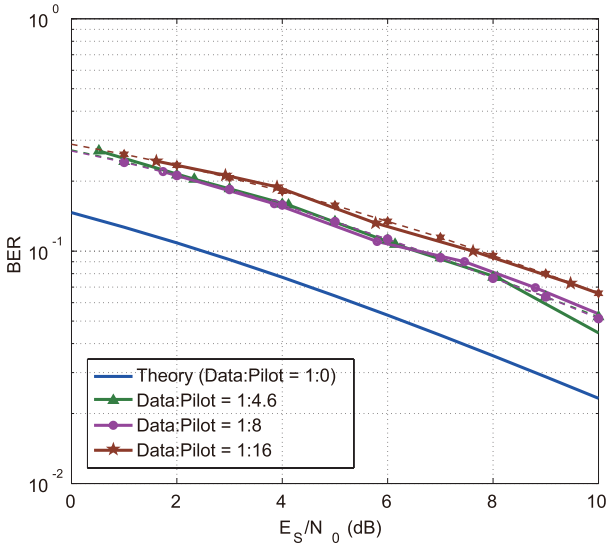

(b) Power ratio of (1:4.6), (1:8), and (1:16).

Fig. 16 BER vs. E_s/N_0 (Zadoff-Chu sequence, Indoor Residencial A channel model).

4. Conclusions

In this paper, the new frame format with OFDM modulation in which data symbols are orthogonally multiplexed with the preamble symbols in the frequency domain is proposed. Two preamble sequences that are based on the IEEE802.11g short preamble sequence and the Zadoff-Chu sequence are employed. The frequency spectrum of the 11g short preamble has a margin at the channel edge to the spectrum mask specified in the IEEE802.11g standard. On the other hand, the frequency spectrum of the Zadoff-Chu sequence based preamble spans over the whole spectrum mask and it can carry 6/5 times more data symbols. The probability of timing synchronization has been evaluated on different channel models through the experiments.

It has been shown through the experiments that there is about 3 or 4 dB deterioration in timing synchronization performance with the proposed preambles as compared to the conventional preamble sequences without data symbol multiplexing. However, the synchronization performance of the proposed scheme shows almost the same synchronization probability as the conventional scheme at E_s/N_0 of more than 8 dB on multipath channel models.

Furthermore, the transmit signal with various power ratios between data and pilot symbols has been evaluated. It

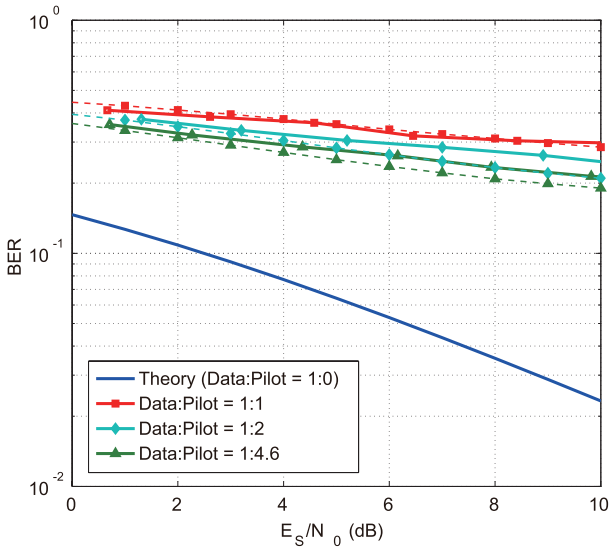

(a) Power ratio of (1:1), (1:2), and (1:4.6).

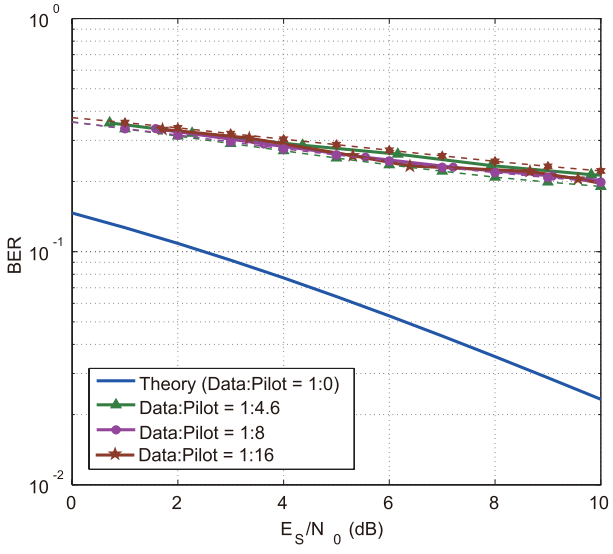

(b) Power ratio of (1:4.6), (1:8), and (1:16).

Fig. 17 BER vs. E_s/N_0 (Zadoff-Chu sequence, Indoor Office C channel model).

has been shown through the experiments that the best BERs are realized with the power ratios of $(P_d : P_p) = (1 : 4.6)$ for the 11g short preamble sequence and $(P_d : P_p) = (1 : 4.6)$ or $(1 : 8)$ for the Zadoff-Chu sequence. This difference comes from the intervals between the pilot subcarriers.

It has also been shown that the synchronization performance of the proposed frame formats suffers from the paths with the large delays on the Indoor Office C channel model. It is required to combine other countermeasures in the physical layer as well as in the protocol layer.

Acknowledgment

The authors would like to thank Mr. T. Kitano in Sanada Lab. for writing the code for the numerical results obtained through computer simulation.

References

[1] J. Kim, J. Lee, J. Kim, and J. You, "M2M service platforms: Survey, issues, and enabling technologies," IEEE Communications Surveys and Tutorials, vol.16, no.1, pp.61–76, 2014.
[2] H.L. Goh, K.K. Tan, S. Huang, and C.W. de Silva, "Development of bluewave: A wireless protocol for industrial automation," IEEE Trans. Industrial Informatics, vol.2, no.4, pp.221–230, Nov. 2006.
[3] G. Habib, J. Petin, and T. Divoux, "Dynamic adaptation of IEEE 802.11e priorities for improving temporal performance and safety of a wireless networked discrete control system," IEEE International Workshop on Dependable Control of Discrete Systems, pp.148–153, June 2011.
[4] H. Okui, M. Suzuki, D. Lee, and H. Morikawa, "A demodulation algorithm of preambleless OFDM system for real-time wireless control networks," IEICE Technical Report, SR2012-39, Oct. 2012.
[5] H. Okui, M. Suzuki, D. Lee, S. Ishida, and H. Morikawa, "Preambleless TDD/TDMA OFDM system for real-time wireless control networks," ACM SenSys 2012, pp.369–370, Nov. 2012.
[6] B. Ai, Z. Yang, C. Pan, J. Ge, Y. Yang, and Z. Lu, "On the synchronization techniques for wireless OFDM systems," IEEE Trans. Broadcast., vol.52, no.2, pp.236–244, June 2006.
[7] P. Stenumgaard, J. Chilo, P. Ferrer-Coll, and P. Angskog, "Challenges and conditions for wireless machine-to-machine communications in industrial environments," IEEE Commun. Mag., vol.51, no.5, pp.187–192, June 2013.
[8] M. Morikura, "Next generation IEEE 802.11 based wireless LAN realizing M2M wireless networks," IEICE Technical Report, CS2012-84, Dec. 2012.
[9] IEEE 802.11g-Part 11: Wireless LAN Medium Access Control (MAC) and Physical Layer (PHY) specifications; High-speed Physical Layer in the 2.4 GHz Band.
[10] K. Tan, J. Zhang, J. Fang, H. Liu, Y. Ye, S. Wang, Y. Zhang, H. Wu, W. Wang, and G.M. Voelker, "Sora: High performance software radio using general purpose multi-core processors," Communications of the Association for Computing Machinery, vol.54, no.1, pp.99–107, Jan. 2011.
[11] T. Yan-bo and G. Wan-Cheng, "Symbol synchronization algorithm based on pseudo-superimposed Zadoff-Chu in advanced-LTE," 2009 Asia-Pacific Conference on Information Processing, pp.140–143, July 2009.
[12] K.-W. Yip, Y.-C. Wu, and T.-S. Ng, "Design of multiplierless correlators for timing synchronization in IEEE 802.11a wireless LANs," IEEE Trans. Consum. Electron., vol.49, no.1, pp.107–114, Feb. 2003.
[13] M.G. Laflin, "Draft final technical report on RF channel characterization and system deployment modeling," Joint Technical Committee, JTC (AIR)/94.08.01-065R4, 1994.
[14] J. Heiskala and J. Terry, OFDM Wireless LANs: A Theoretical and Practical Guide, Indianapolis, Sams Publishing, 2001.
[15] R. Takai, S. Uchida, A. Sato, M. Inamolri, and Y. Sanada, "Experimental investigation of signal sensing with overlapped FFT based energy detection under the existence of fixed distortion component," IEICE Technical Report, SR2013-19, May 2013.

Yuki Tanaka was born in Hyogo, Japan in 1986. He received his B.E. degree in electronics engineering from Keio University, Japan in 2012. Since April 2012, he has been a graduate student in School of Integrated Design Engineering, Graduate School of Science and Technology, Keio University. His research interests are mainly concentrated on software defined radio.

Yukitoshi Sanada was born in Tokyo in 1969. He received his B.E. degree in electrical engineering from Keio University, Yokohama Japan, his M.A.Sc. degree in electrical engineering from the University of Victoria, B.C., Canada, and his Ph.D. degree in electrical engineering from Keio University, Yokohama Japan, in 1992, 1995, and 1997, respectively. In 1997 he joined the Faculty of Engineering, Tokyo Institute of Technology as a Research Associate. In 2000 he joined Advanced Telecommunication Laboratory, Sony Computer Science Laboratories, Inc, as an associate researcher. In 2001 he joined Faculty of Science and Engineering, Keio University, where he is now a professor. He received the Young Engineer Award from IEICE Japan in 1997. His current research interest are in software defined radio, cognitive radio, and OFDM systems.